

Performance of dissipative dielectric elastomer generators

Choon Chiang Foo, Soo Jin Adrian Koh, Christoph Keplinger, Rainer Kaltseis, Siegfried Bauer et al.

Citation: *J. Appl. Phys.* **111**, 094107 (2012); doi: 10.1063/1.4714557

View online: <http://dx.doi.org/10.1063/1.4714557>

View Table of Contents: <http://jap.aip.org/resource/1/JAPIAU/v111/i9>

Published by the [American Institute of Physics](#).

Related Articles

Thermoacoustic compression based on alternating to direct gas flow conversion

J. Appl. Phys. **111**, 094905 (2012)

Mixing properties of coaxial jets with large velocity ratios and large inverse density ratios

Phys. Fluids **24**, 055101 (2012)

Towards constructing multi-bit binary adder based on Belousov-Zhabotinsky reaction

J. Chem. Phys. **136**, 164108 (2012)

A low-voltage high-speed electronic switch based on piezoelectric transduction

J. Appl. Phys. **111**, 084509 (2012)

Highly precise and compact ultrahigh vacuum rotary feedthrough

Rev. Sci. Instrum. **83**, 035106 (2012)

Additional information on J. Appl. Phys.

Journal Homepage: <http://jap.aip.org/>

Journal Information: http://jap.aip.org/about/about_the_journal

Top downloads: http://jap.aip.org/features/most_downloaded

Information for Authors: <http://jap.aip.org/authors>

ADVERTISEMENT



IBD Optical Film Quality at PVD Rates

Advanced Optical Thin Films

Wide Range of Applications

Superior Throughput and Repeatability

SPECTOR-HT ION BEAM DEPOSITION SYSTEMS

Veeco

Innovation. Performance. Brilliant.

www.veeco.com/spectorht

Performance of dissipative dielectric elastomer generators

Choon Chiang Foo,^{1,2} Soo Jin Adrian Koh,^{2,3} Christoph Keplinger,^{1,4} Rainer Kaltseis,⁴ Siegfried Bauer,⁴ and Zhigang Suo^{1,a)}

¹*School of Engineering and Applied Sciences, Kavli Institute for Nanobio Science and Technology, Harvard University, Cambridge, Massachusetts 02138, USA*

²*Institute of High Performance Computing, 1 Fusionopolis Way, #16-16 Connexis, Singapore 138632, Singapore*

³*Engineering Science Programme and Department of Civil and Environmental Engineering, National University of Singapore, Kent Ridge, Singapore 119260, Singapore*

⁴*Soft-Matter Physics Department, Johannes Kepler University Linz, A-4040 Linz, Austria*

(Received 4 March 2012; accepted 9 April 2012; published online 10 May 2012)

Dielectric elastomer generators are high-energy-density electromechanical transducers. Their performance is affected by dissipative losses. This paper presents a theoretical analysis of a dielectric elastomer generator with two dissipative processes: viscoelasticity and current leakage. Conversion cycles are shown to attain steady-state after several cycles. Performance parameters such as electrical energy generated per cycle, average power, and mechanical to electrical energy conversion efficiency are introduced. Trade-offs between large electrical energy and power output and poor conversion efficiency are discussed. Excessive current leakage results in negative efficiency—the dielectric elastomer generator wastes energy instead of generating it. The general framework developed in this paper helps in the design and assessment of conversion cycles for dissipative dielectric elastomer generators. © 2012 American Institute of Physics. [<http://dx.doi.org/10.1063/1.4714557>]

I. INTRODUCTION

A membrane of a dielectric elastomer, sandwiched between two compliant electrodes, is a deformable capacitor. When the elastomer is subject to voltage, it reduces its thickness and expands its area—the elastomer functions as an actuator.^{1,2} When a pre-stretched and pre-charged elastomer is allowed to contract under the open-circuit conditions, the voltage across the electrodes is boosted—the elastomer functions as a generator.³

Dielectric elastomer generators (DEGs) are highly deformable, lightweight, low in cost, resistant to corrosion and have a high specific energy of conversion.^{3,5} DEGs were designed to harvest energy from human motion^{5,6} and ocean waves.^{5,7} DEGs with specially designed self-priming circuits allow energy to be harvested within a small, portable unit.^{8–10} Reported values of specific energy conversion range from 0.133 to 400 mJ/g.^{3,5,11} Theoretical estimates indicated electrical energy per cycles as high as 1.7 J/g for acrylic elastomers,⁴ more than an order of magnitude higher than existing technologies such as piezoelectric and electromagnetic materials.^{5,12}

However, there is no such a thing like perfect dielectric. Dielectric elastomers suffer from dissipative processes; in this paper, we discuss the effect of viscoelasticity and leakage currents on the performance of DEGs. Experiments have shown that viscoelasticity and current leakage significantly affect the energy conversion performance of dielectric elastomer transducers.^{9,13–16} Here, we develop a theoretical framework to analyze how viscoelasticity and current leakage affect the performance of a dissipative dielectric elastomer generator, similar to our previous work on dielectric

elastomer actuators.¹⁶ We first show that conversion cycles in DEGs reach steady-state conditions after several cycles. This allows us to represent cycles in work conjugate plots. We then introduce performance parameters of DEGs: electrical energy generated per cycle, average power output, and mechanical to electrical energy conversion efficiency. We show that DEGs can waste energy instead of generating it, under conditions of excessive leakage currents when operated close to the material limits. We also introduce contour plots for the performance parameters of generators, which help in the design and assessment of cycles. In particular, we analyze how optimal outputs may be achieved under given specific operating conditions.

II. MODEL OF DISSIPATIVE DIELECTRIC ELASTOMERS

This section summarizes the model of dissipative dielectric elastomers.¹⁶ Consider a membrane of a dielectric elastomer sandwiched between compliant electrodes (Fig. 1). The electrodes are assumed to have negligible electrical resistance and mechanical stiffness. In the reference state, the elastomer is undeformed and uncharged. In a deformed state, the membrane is subject to an equal-biaxial force P and is connected to a voltage source Φ through a conducting wire. The dimension of the elastomer changes from L to l in both in-plane directions, while its thickness reduces from H to h . The elastomer is taken to be viscoelastic and an imperfect insulator. The voltage source is connected to the membrane through a conducting wire, in which the current is i . The magnitude of the charge on the electrodes is Q_p , and the current through the membrane is i_{leak} . To focus on dissipation due to the elastomer, we further assume that the conducting wire and the compliant electrodes are perfect conductors, so

^{a)} suo@seas.harvard.edu.

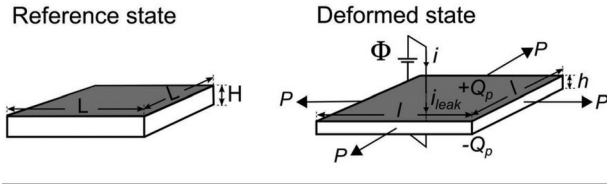


FIG. 1. A membrane of a dielectric elastomer is sandwiched between compliant electrodes. In the reference state, unstretched and uncharged, the membrane is of thickness H and area L^2 . In a deformed state, subject to equal-biaxial forces P and voltage Φ , the membrane is of thickness h and area l^2 . The dielectric elastomer is viscoelastic and leaks current. The voltage is connected to the membrane through a conducting wire, in which the current is i . The magnitude of the charge on the electrodes is Q_p , and the current leaking through the membrane is i_{leak} .

that the current flows from the voltage source to the electrodes with no losses. Define the stretch as $\lambda = l/L$, the stress as $\sigma = P/(lh)$, the electric displacement as $D = Q_p/l^2$, the electric field as $E = \Phi/h$, and the leakage current density as $j_{leak} = i_{leak}/l^2$. The elastomer is assumed to be incompressible so that $h = H\lambda^{-2}$.

We model current leakage by representing the dielectric elastomer as a capacitor in parallel with a conductor (Fig. 2(a)). Let Q be the total amount of charge transported through the conducting wire, Q_p be the magnitude of the positive and negative charges on the two electrodes that polarize the membrane, and Q_{leak} be the charge that leaks through the membrane. The conservation of charge requires that

$$Q = Q_p + Q_{leak}. \quad (1)$$

The electric displacement relates to the electric field by $D = \epsilon E$, where permittivity of the elastomer ϵ is assumed to be independent of deformation.¹⁷ We may relate Q_p to Φ as

$$Q_p = \frac{\epsilon L^2 \lambda^4}{H} \Phi. \quad (2)$$

Equation (2) is the capacitive relation that connects the charge on the electrodes to the voltage. The membrane is a deformable capacitor: the capacitance varies with the stretch as λ^4 .

The amount of Q_{leak} that flows through the membrane per unit time is the leakage current (i_{leak}). Leaked charges

may be a result of the transport of electrons, ions, or both.^{18,19} The onset and amount of leakage current is often linked to the presence of impurities and imperfections.^{18,19} i_{leak} may not be easily measured and is often inferred from Eq. (1). Differentiating Eq. (1) with respect to time, we write

$$i = \frac{dQ_p}{dt} + i_{leak}, \quad (3)$$

where i_{leak} may be inferred from the difference of measurable quantities i , and the rate of change of polarizing charge dQ_p/dt , which is related to measurable quantities of Φ , λ , ϵ , and H in Eq. (2). Equation (3) also defines the current flow through the electrical circuit shown in Fig. 2(a).

Recent experiments have reported that the conductivity for VHB 4910 increases exponentially under increasing electric field.²⁰ We relate the leakage current density j_{leak} to the electric field E as

$$j_{leak} = \sigma_c(E)E. \quad (4)$$

We assume that the conductivity varies exponentially with the electric field¹⁶

$$\sigma_c(E) = \sigma_0 \exp\left(\frac{E}{E_B}\right), \quad (5)$$

where σ_0 is the conductivity at small electric fields, and E_B is an empirical constant with the same dimension as the electric field. When $E \ll E_B$, the elastomer approximates an Ohmic conductor, i.e., $j_{leak} \approx \sigma_0 E$. As $E \rightarrow E_B$, the conductivity increases exponentially.²⁰

The RC time constant in a resistor-capacitor circuit is defined by the ratio between the permittivity and the conductivity of the dielectric

$$\tau_{RC} = \epsilon/\sigma_c. \quad (6)$$

Note that σ_c in Eq. (6) is a highly nonlinear function of E . Because the dielectric typically operates under high electric fields, we assume the conductivity is taken at 90% of the electrical breakdown field to estimate τ_{RC} . Here, we assume the electrical breakdown field to be 230 MV/m,^{4,21} which results in $\tau_{RC} = 7$ s.

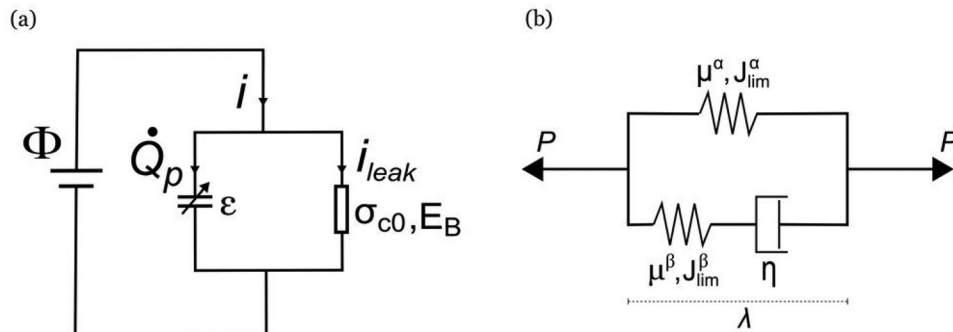


FIG. 2. Schematic representations of two dissipative processes: current leakage and viscoelasticity. (a) Current leakage is modeled by representing the membrane as parallel capacitor and resistor. By the principle of the conservation of charge, the current in the conducting wire i is the sum of the rate of the charge on the capacitor \dot{Q}_p and the leakage current through the resistor i_{leak} . (b) Viscoelasticity is represented by a rheological model of two parallel units: the top unit consists of spring α , and the bottom unit consists of spring β in series with a dashpot.

Viscoelastic dielectrics have recently been studied theoretically using rheological models of springs and dashpots.^{16,22,23} Here, we adopt a model of two polymer networks connected in parallel (Fig. 2(b)). One network consists of a spring α , and the other network consists of another spring β connected in series with a dashpot. Experiments have shown that elastomers stiffen significantly when highly stretched.²¹ This may be due to the finite contour length of the polymer chains, which imposes a limit stretch.²⁴ To account for this stiffening effect, we characterize both springs using the Gent model; μ^α and μ^β are the shear moduli of the two springs, and J_{lim}^α and J_{lim}^β are the constants related to the limiting stretches of the two springs. Subject to a force, the networks deform by a stretch λ . By geometry, the spring α deforms by stretch λ . For the bottom network, the spring β deforms by stretch λ^e , and the dashpot deforms by stretch ξ . The total stretch in the bottom network is given by $\lambda^e \xi$, which must be equal to λ . We write

$$\sigma + \varepsilon E^2 = \frac{\mu^\alpha (\lambda^2 - \lambda^{-4})}{1 - (2\lambda^2 + \lambda^{-4} - 3)/J_{\text{lim}}^\alpha} + \frac{\mu^\beta (\lambda^2 \xi^{-2} - \xi^4 \lambda^{-4})}{1 - (2\lambda^2 \xi^{-2} + \xi^4 \lambda^{-4} - 3)/J_{\text{lim}}^\beta}. \quad (7)$$

Equation (7) gives the equation-of-state for a viscoelastic dielectric elastomer. The left-hand side of Eq. (7) is the applied stress (σ) and Maxwell stress (εE^2), balanced by the stresses in the springs on the right-hand side.

We model the dashpot as a Newtonian fluid. From Fig. 2(b), considering equilibrium of forces in the bottom network, the stress in the dashpot must be equal to that in spring β . This stress is given as the last term in Eq. (7). The rate of deformation in the dashpot is described by $\xi^{-1} d\xi/dt$. We relate the rate of deformation in the dashpot to the stress on the dashpot and write

$$\frac{d\xi}{dt} = \frac{\mu^\beta J_{\text{lim}}^\beta \xi (\xi^4 \lambda^{-4} - \lambda^2 \xi^{-2})}{6\eta (2\lambda^2 \xi^{-2} + \xi^4 \lambda^{-4} - 3 - J_{\text{lim}}^\beta)}, \quad (8)$$

where η is the viscosity of the dashpot. The viscoelastic relaxation time is defined by the ratio of the viscosity of the dashpot and the modulus of spring β

$$\tau_V = \eta/\mu^\beta. \quad (9)$$

Experiments have suggested that very-high-bond (VHB) elastomer possesses multiple relaxation times, which range from a few seconds to hundreds of seconds or even longer.^{25,26} To illustrate essential ideas, we shall only consider a single relaxation time in our analysis, but note that our model may be extended to accommodate multiple relaxation times.

The system of equations evolves the state of the membrane in time.¹⁶ The membrane is a transducer of two external degrees of freedom. The mechanical degree of freedom is characterized by a pair of work-conjugate variables: the force P and the length l . The electrical degree of freedom is characterized by another pair of work-conjugate variables: the voltage Φ and the charge Q . These four variables are

typically measured experimentally and are known as external variables. Any two of the four external variables can be used to specify a state of the transducer. To fully specify a state of the transducer, however, we also need to know the internal variables that characterize the progression of the dissipative processes, such as the stretch of the dashpot ξ and the charge on the electrodes Q_p . In simulation, we prescribe two of the external variables independently as functions of time and use the system of equations to evolve the other two external variables and all the internal variables in time.

III. CYCLE OF ENERGY CONVERSION

Dielectric elastomer generators have been designed to operate in cycles of various kinds.^{4,5,14,15,27} Here, we consider a dielectric elastomer generator that couples a dielectric membrane to the external circuits via a three-way switch (Fig. 3). Two reservoirs of charges are represented a battery of a low voltage Φ_L and a battery of a high voltage Φ_H . A cycle consists of two constant-voltage processes and two open-circuit processes (Fig. 4). In the constant-voltage process A→B, the switch connects the membrane to the battery of the low voltage Φ_L , the force stretches the membrane, and the battery of the low voltage Φ_L supplies charges to the electrodes. In the open-circuit process B→C, the switch disconnects the membrane from either battery, the mechanical force is partially released to make the membrane contract in length and increase in thickness, and the voltage between the two electrodes increases. In the constant-voltage process C→D, the switch connects the membrane to the battery of the high voltage Φ_H , the force is further released to make the membrane contract in length and increase in thickness, and the membrane pumps charges to the battery of the high voltage Φ_H . In the open-circuit process D→A, the switch disconnects the membrane from either battery, the mechanical force stretches the membrane, and the voltage between the two electrodes decreases. During the cycle, charge may also flow as the leakage current i_{leak} through the membrane.

The cycle can be represented in the force-length diagram and voltage-charge diagram (Fig. 5). A point in either diagram

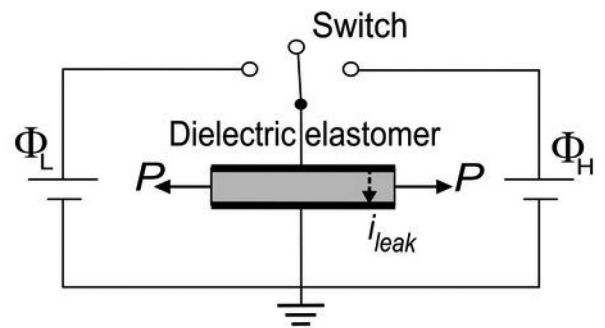


FIG. 3. A dielectric elastomer generator uses mechanical work to pump electric charge from a reservoir of low voltage to a reservoir of high voltage. The mechanical work is done by applying a force P on a membrane of a dielectric elastomer. The two reservoirs of charges are represented by a battery of low voltage Φ_L and a battery of high voltage Φ_H . A three-way switch can connect the membrane to either battery in a constant-voltage condition or disconnect the membrane from both batteries and keep it in an open-circuit condition.

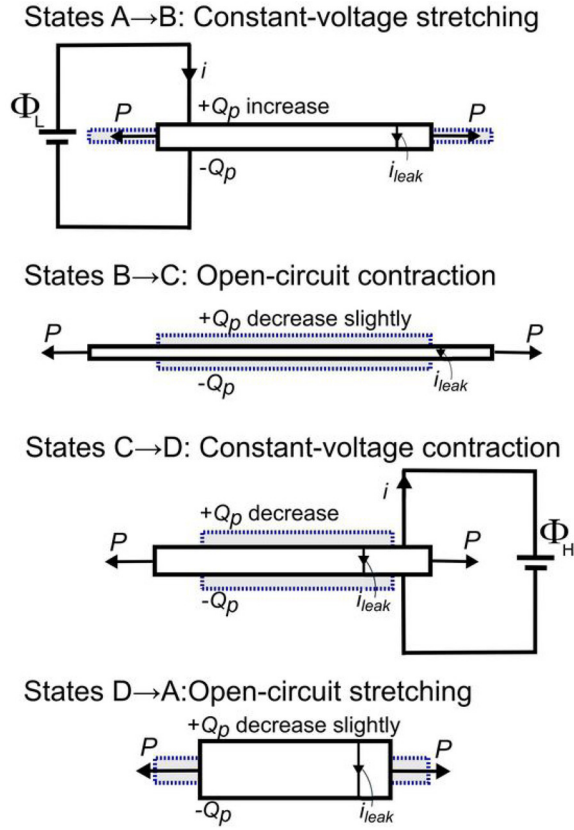


FIG. 4. (Color online) A dielectric elastomer generator operates in a cycle of four processes. The solid lines indicate the membrane at the beginning of a process, and the dashed lines indicate the membrane at the end of the process. In the constant-voltage process A→B, the switch connects the membrane to the battery of the low voltage Φ_L , which supplies charges to the electrodes while the force stretches the membrane. In the open-circuit process B→C, the switch disconnects the membrane from either battery, the mechanical force is partially released to make the membrane contract in length and increase in thickness, and the voltage between the two electrodes increases. In the constant-voltage process C→D, the switch connects the membrane to the battery of the high voltage Φ_H , which receives charge from the membrane as the force is released to make the membrane contract in length and increase in thickness. In the open-circuit process D→A, the switch disconnects the membrane from either battery, the mechanical force stretches the membrane, and the voltage between the two electrodes decreases.

denotes a state, a line denotes a process, and a contour denotes a cycle. Dotted lines represent a cycle for a generator without loss, while solid lines represent a cycle for a generator with current leakage and viscoelastic relaxation. The area bounded by the rectangle A'B'C'D'A' in the voltage-charge diagram gives the electrical energy converted by the generator without loss, which is exactly two times that of the region bounded by the dotted lines in the force-length diagram. This cycle was described in a previous work^{4,27} and demonstrated experimentally.¹⁵ This cycle when represented on the voltage-charge diagram is reminiscent of the Carnot cycle when represented on the temperature-entropy diagram.²⁸ The Carnot cycle sets ideal operating conditions, as practical devices are never as efficient as the Carnot cycle. For instance, the efficiency of heat engines is limited by the rate of heat transfer to and from the working substance.²⁹ Similarly, subject to cyclic loadings, the performance of a dielectric elastomer generator is affected by dissipative processes.^{9,13,15}

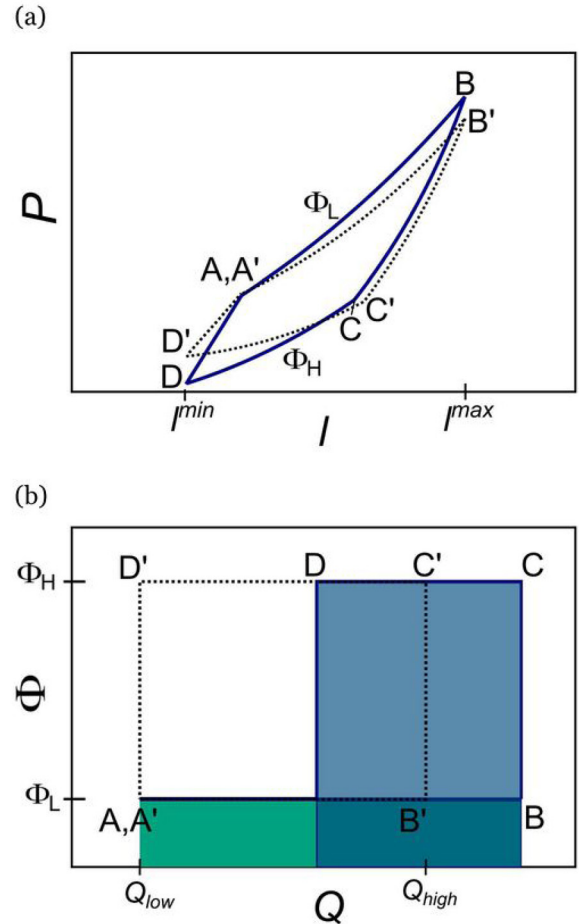


FIG. 5. (Color online) A cycle represented in (a) force-length diagram and (b) voltage-charge diagram. Dotted lines represent a cycle for a generator without loss, while solid lines represent a cycle for a generator with current leakage and viscoelastic relaxation. The area enclosed by the dotted lines in (b) is two times that in (a) due to equal-biaxial deformation. The area enclosed by the solid line in (a) gives the input mechanical energy. The area under A → B gives the electrical energy transferred from the battery of the low voltage Φ_L to the membrane. The area under C → D gives the electrical energy transferred from the membrane to the battery of the high voltage Φ_H .

The cycle for the dissipative generator is similar to that of the generator without loss, except for three differences. First, due to viscoelasticity, the dissipative generator requires a few cycles to achieve a steady-state, a point to be elaborated later in Sec. IV. Fig. 5 shows only the steady-state cycle. Second, the viscoelastic loss enlarges the area of the cycle in the force-length diagram. Third, due to leakage charge Q_{leak} , the total charge at state B is greater than Q_{high} (Fig. 5(b)). Electrical work is done *on* the membrane in the direction of *increasing* Q . The amount of electrical work done on the membrane is the total area bounded under the line AB. Conversely, electrical work is done *by* the membrane in the direction of *reducing* Q . The difference between the work done *by* the membrane (C→D) and the work done *on* the membrane (A→B) gives the net energy produced by the membrane. Because of leakage charge, the initial and final states in the Φ - Q plane will not meet after completion of one cycle.

In simulating the cycle, we prescribe an input signal of stretch-time (Fig. 6). In this signal, we prescribe an initial

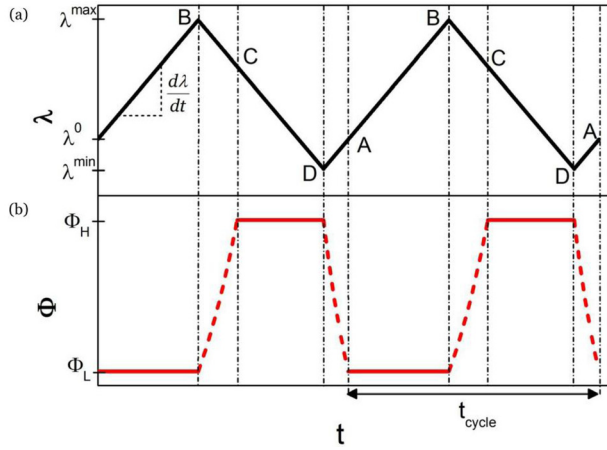


FIG. 6. (Color online) Two of the four external variables can be prescribed independently as functions of time. (a) The stretch is applied at a constant rate. (b) The switch connects the membrane to either battery (solid lines) or disconnects the membrane from both batteries (dashed lines).

pre-stretch λ^0 before the start of the first cycle. A long time is allowed to elapse, so as to enable the stress in the membrane to equilibrate with λ^0 , before the energy conversion cycle begins. For all cycles, we prescribe the maximum stretch λ^{\max} and minimum stretch λ^{\min} at states B and D, respectively. We also prescribe a constant magnitude for the stretch rate $d\lambda/dt$ during all steps in this cycle. The period of the cycle is

$$t_{\text{cycle}} = \frac{2(\lambda^{\max} - \lambda^{\min})}{d\lambda/dt}. \quad (10)$$

We also prescribe Φ_L and Φ_H when the switch connects the membrane to either battery.

We define three indices of performance: specific net electrical energy generated per cycle in J/g (Y), specific power generated per cycle in W/g (ψ), and the mechano-

electrical conversion efficiency (η_{me}). For a generator, the mechanical work done per cycle is integrated over the cycle on the force-length diagram

$$W_{\text{mech}} = 2 \int P d\lambda. \quad (11)$$

All integrals are taken over a steady-state cycle. The factor of 2 results from equal-biaxial deformation. The electrical energy generated per cycle is integrated over the cycle on the voltage-charge diagram

$$W_{\text{ele}} = - \int \Phi dQ. \quad (12a)$$

The negative sign is used to conform to the convention that $W_{\text{ele}} > 0$ if the cycle generates electrical energy. Recall the conservation of charge, $dQ = dQ_p + dQ_{\text{leak}}$; the electrical energy generated can also be expressed as

$$W_{\text{ele}} = - \int \Phi dQ_p - \int \Phi dQ_{\text{leak}}. \quad (12b)$$

The generator may produce negative electrical energy, if the charge leakage Q_{leak} is excessive—that is, the generator dissipates more energy than it generates. This behavior should be avoided.

Define the specific electrical energy generated per cycle as

$$Y = \frac{W_{\text{ele}}}{\rho L_1 L_2 L_3}, \quad (13)$$

where ρ is the mass density of the elastomer. One strives to maximize Y , so as to produce a maximal amount of energy with minimal amounts of material. Define the specific power per cycle as

$$\Psi = \frac{Y}{t_{\text{cycle}}}. \quad (14)$$

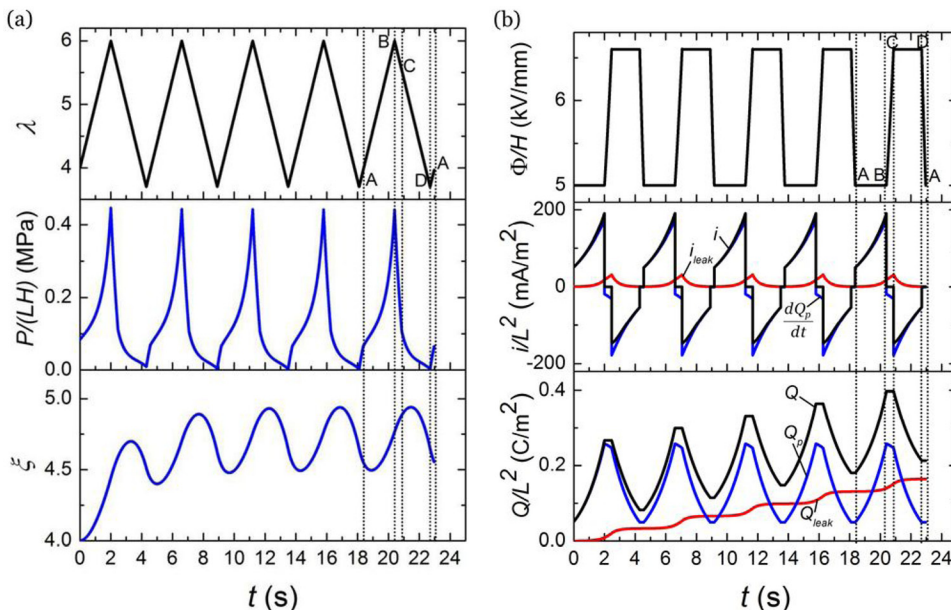


FIG. 7. (Color online) Variables as functions of time. (a) Mechanical variables: stretch λ , the nominal stress P/LH , the stretch in the dashpot ξ . (b) Electrical variables: the nominal electric field Φ/H , the nominal current density supplied by the batteries i/L^2 , the nominal current density that charges the elastomer $(dQ_p/dt)/L^2$, the nominal leakage current density i_{leak}/L^2 , and their corresponding nominal charge densities Q/L^2 . The system achieves a steady-state after about four cycles. The period of each cycle is $t_{\text{cycle}} = 4.6$ s.

Equation (14) allows one to adapt the operation of a DEG based on a given power rating, by selecting an appropriate combination of Y and t_{cycle} . One may also wish to enhance the specific power per cycle by speeding up the cyclic operation.⁵ Define the mechano-electrical conversion efficiency η_{me} as

$$\eta_{me} = \frac{W_{ele}}{W_{mech}}. \quad (15)$$

A generator without loss operates at $\eta_{me} = 1$. On the other hand, when $W_{ele} < 0$, the system operates at negative efficiency; the generator is wasting energy instead of generating it.

In the dissipative generator, energy is lost due to viscoelasticity and charge leakage. For viscoelastic relaxation, the elastomer dissipates energy through the work done on the dashpot. As mentioned earlier, the stress acting on the dash-

pot σ^β is the same stress that acts on the spring β (Eq. (7)), and we denote the nominal stress as: $s^\beta = \sigma^\beta / \xi$. The viscous loss W_{visc} in a cycle is given as

$$W_{visc} = 2L^2H \int s^\beta d\xi. \quad (16)$$

Similarly, the dissipated energy due to current leakage is defined as

$$W_{leak} = \int \Phi dQ_{leak}. \quad (17)$$

By the conservation of energy, the input energy must be equal to the output energy and losses

$$W_{mech} = W_{ele} + W_{visc} + W_{leak}. \quad (18)$$

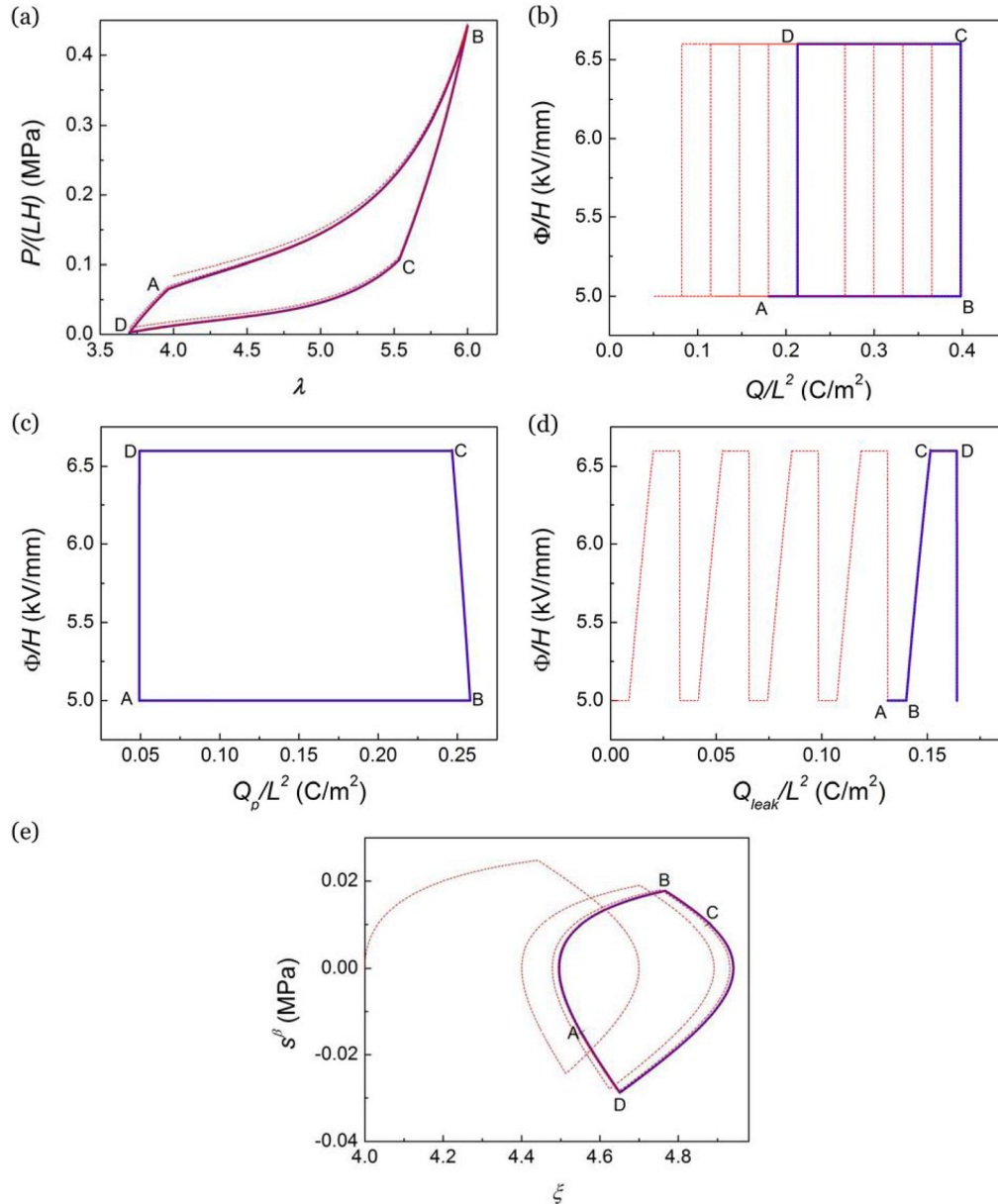


FIG. 8. (Color online) Cycles are represented in diagrams of work-conjugating variables. The dotted line depicts the response from the start of the cycle, while the solid line depicts the steady-state cycle.

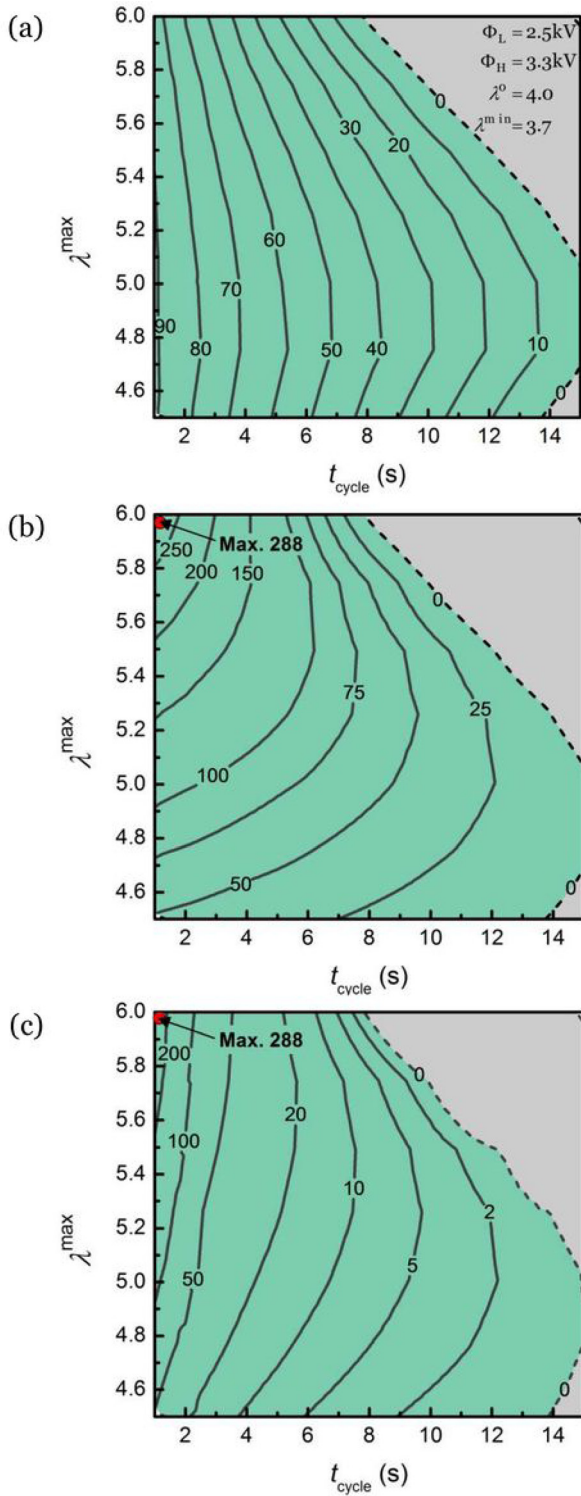


FIG. 9. (Color online) Contour plots showing the effect of maximum stretch (λ^{\max}) and period (t_{cycle}) on the performance of a generator. (a) Mechano-electrical energy conversion efficiency in percentage; (b) specific electrical energy generated per cycle in mJ/g; and (c) average specific power in mW/g. In these plots, initial pre-stretch (λ^0), minimum stretch (λ^{\min}), and input and output voltages (Φ_L and Φ_H) are fixed.

IV. CYCLE PERFORMANCE OF A DISSIPATIVE DIELECTRIC ELASTOMER GENERATOR

Polyacrylate VHB elastomer has been used extensively to develop dielectric elastomer generators.^{3–5,7–11,15,27} We

select this material for our analysis and fitted the material parameters in Eq. (7) based on existing experimental data,²⁵ as follows: $\mu^\alpha = 25$ kPa, $\mu^\beta = 70$ kPa, $J_{\text{lim}}^\alpha = 90$, and $J_{\text{lim}}^\beta = 30$. To illustrate the effect of viscoelasticity on the energy conversion performance of a dielectric elastomer generator, we assume a single relaxation time of $\tau_V = 3$ s,²⁵ comparable to the time scale of operation for the generator.⁵ We assume the elastomer to be lightly crosslinked, which polarizes like a polymer melt. As such, the dielectric permittivity ϵ is negligibly affected by deformation.³⁰ Experiments suggest that $\epsilon = 4.5\epsilon_0$.²¹ We neglect dielectric relaxation in our analysis. Parameters for the current leakage model in Eq. (5) have been previously fitted to experiments,^{16,31} where $\sigma_{c0} = 3.23 \times 10^{-14}$ S/m and $E_B = 40$ MV/m.

As mentioned before, of the four external variables, the force P , length l , voltage Φ , and charge Q , any two can be prescribed independently as functions of time. The other two external variables, along with all the internal variables can be calculated by evolving the system of equations in time. In a simulation, we prescribe $\lambda^0 = 4$, $\lambda^{\max} = 6$, and $\lambda^{\min} = 3.7$, as well as $\Phi_L = 2.5$ kV and $\Phi_H = 3.3$ kV (Fig. 6). The period is $t_{\text{cycle}} = 4.6$ s. We show the response of the generator in time-history plots (Fig. 7) and in diagrams of various work-conjugating variables (Fig. 8). Due to viscoelasticity, the generator may require a few cycles for the mechanical response to achieve steady-state. This implies that the states in the force-length diagram do not form a closed loop, until steady-state is attained (Fig. 8(a)). The stress-stretch plot of the dashpot clearly exhibits this fact (Fig. 8(e)). In our calculations, steady-state was typically attained after four to five cycles (Fig. 7). Steady-state may be attained for the first cycle only when the elastomer exhibits elastic mechanical response—when the cycle time of the generator is much faster, or much slower than the viscoelastic time scale, defined in Eq. (9). Due to current leakage, the total charges in the generator will increase after every cycle (Fig. 7(b)). In the voltage-charge diagram, the initial and final states will not meet after completion of one cycle (Fig. 8(b)). By definition of Eq. (1), the sum of the areas in the Φ – Q_p , and the Φ – Q_{leak} diagrams, in the steady state, must be equal to the electrical output by the generator.

In the cycle depicted in Figs. 7 and 8, the specific electrical energy generated per cycle Y is 131 mJ/g, with a specific average power ψ of 28.4 mW/g. The mechano-electrical conversion efficiency for this cycle is 37%. This low efficiency is due to dissipation in the generator. Viscous losses (Fig. 8(e)) increase the amount of mechanical work required to stretch the elastomer, which reduces the efficiency. Charge losses associated with leakage current through the membrane (Fig. 8(d)) significantly affect the efficiency and the specific energy output of the dielectric elastomer generator in three ways. First, these charge losses increase the electrical work input during charging of the elastomer ($A \rightarrow B$). Second, when the generator is operating in the open-circuit condition ($B \rightarrow C$), charge losses result in a slight decrease in the polarizing charges on the electrodes of the elastomer (Fig. 8(c)). If the contraction process is too slow, significant leakage current may result in a very small or even negative voltage boost. Third, charge losses decrease

the net amount of charge that is delivered to the output battery during discharging ($C \rightarrow D$), resulting in lower electrical work output. However, we note that current leakage is somewhat negligible during $D \rightarrow A$, as the voltage across the elastomer drops to Φ_L under low stretch states.

We next illustrate the performance of a generator over a specific range of operating conditions. In this set of calculations, we set $\Phi_L = 2.5$ kV, $\Phi_H = 3.3$ kV, $\lambda^0 = 4$, and $\lambda^{\min} = 3.7$, and study the effect of t_{cycle} and λ^{\max} on the performance. We plot these data on contour plots (Fig. 9). The generator is most efficient in fast cycles with relatively small operating strains (Fig. 9(a)). As the cyclic period increases, the generator becomes less efficient. For slower cycles, the efficiency of the generator also decreases for cycles with higher operating strains. For instance, at $t_{\text{cycle}} \approx 8$ s, the efficiency first increases due to greater conversion energy at increasing strains of operation, before the efficiency decreases from 40% to negative as λ^{\max} increases from 4.8 to 6. At negative efficiency, the generator is not producing any net useful electrical output. Instead of harvesting energy, the generator is wasting energy. The efficiency drop is due to increased viscous and leakage losses under larger operating strains. Leakage losses still dominate, due to the higher electric fields at large actuation.¹⁶ This observation is also consistent with experimental observations, which show leakage losses significantly limit the efficiency of actuation cycles under large stretches.¹³

In terms of specific energy generated (Fig. 9(b)) and specific power (Fig. 9(c)), the dissipative generator performs better with increasing λ^{\max} for $t_{\text{cycle}} < 7$ s. This is in agreement with our previous finding, which shows that an ideal generator achieves greater specific energy with increasing strains of operation.⁴ However for cycles with $t_{\text{cycle}} > 7$ s, there exists an optimal λ^{\max} , where the specific energy and power attains a peak, before deteriorating as λ^{\max} increases further. Interestingly, the onset of this phenomenon coincides with $t_{\text{cycle}} = 7$ s, which is the estimated RC time constant computed using Eq. (6). This means that the effect of current leakage becomes increasingly pronounced for cycle times

greater than the RC time constant, thereby reducing the energy generated, especially at large strains of operation. In our example, the maximum possible specific energy generated per cycle and specific power are 288 mJ/g and 288 mW/g, respectively, at $\lambda^{\max} = 6$ and $t_{\text{cycle}} = 1$ s (Figs. 9(b) and 9(c)).

The plots in Fig. 9 also indicated an inverse relationship between efficiency and the energy generated. That is, the generator may convert energy very efficiently, but generate a small specific energy and power. Nevertheless, one may then use these plots to design a dielectric elastomer generator, based on a given set of environmental constraints. For example, if we assume a typical period of 4 s for generators deployed to harvest energy from ocean waves,³² the generator should operate with a maximum stretch $\lambda^{\max} = 6$, so as to extract the highest specific energy and power output. On the other hand, if maximum conversion efficiency is desired, the generator should operate at $\lambda^{\max} = 5$. Previously, a specific electrical energy generated of 125 mJ/g had been reported for prototype buoy generators operating at 0.3 Hz (Ref. 32). Small scale parasitic power generators, which capture energy from sources such as human activity,^{5,6,11} may have different optimization goals from large scale generators used to harvest energy from renewable sources such as wind or ocean waves. Still, we may design the generator for different applications using the contour plots. We further note that the actual specific energy and power densities of any generator also depend on its configuration, material parameters, operating conditions, and electronic circuit design. The aim of this paper is not to compare quantitatively with published results, but to present a method to evaluate and design a dielectric elastomer generator. More realistic and accurate contour plots may be produced when more experimental data become available.

To be more specific on losses, we plot Fig. 10 for $\lambda^0 = 4$, $\lambda^{\max} = 6$, and $\lambda^{\min} = 3.7$, and $\Phi_L = 2.5$ kV and $\Phi_H = 3.3$ kV. Figure 10(a) shows the mechanical input (W_{mech}) and electrical output (W_{ele}) over a range of t_{cycle} , and Fig. 10(b) shows the losses from viscoelasticity (W_{visc}) and

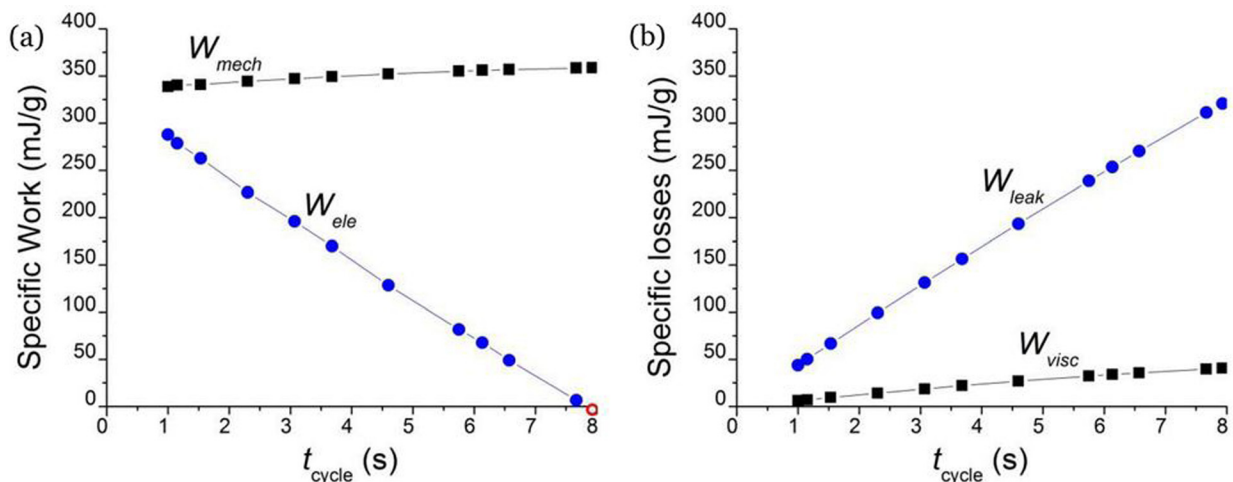


FIG. 10. (Color online) Effect of period on the specific work and losses of a generator operating under $\lambda^0 = 4$, $\lambda^{\max} = 6$, and $\lambda^{\min} = 3.7$, and $\Phi_L = 2.5$ kV and $\Phi_H = 3.3$ kV. (a) Net electrical output and mechanical input work. (b) Viscous and leakage losses.

current leakage (W_{leak}) in isolation. As t_{cycle} increases, viscous losses build up. This leads to a higher mechanical input work (Fig. 10(a)), with more work expended through viscous dissipation, thereby lowering the conversion efficiency (Fig. 9(a)). Despite the viscoelastic nature of VHB,^{9,13,15} leakage losses increase more substantially and dominate for slower cycles (Fig. 10(b)). This results in a rapidly decreasing net electrical energy generated (Fig. 10(a)) with increasing t_{cycle} . However when t_{cycle} is much smaller than the dissipation time scales, τ_V and τ_{RC} , losses are minimal and the generator may be capable of high specific energy and power densities (Figs. 9(b) and 9(c)). Therefore to achieve an efficient generator with high specific energy and power densities, it may be attractive to operate at cyclic periods faster than the dissipation time scales of the elastomer.

V. CONCLUSION

This paper models dielectric elastomer generators with two dissipative processes: viscoelasticity and current leakage. The generator is modeled as a system of two degrees of freedom and the generation cycle is represented on work-conjugate planes. The area bounded by the contour describing the cycle on the force-displacement plane represents the input mechanical energy, while the corresponding area on the voltage-charge plane gives the generated electrical energy per cycle. Subsequently, the electromechanical efficiency, the specific electrical energy generated per cycle, and the specific average power may be obtained. We determine the steady state response and illustrate the effects of dissipation for generators made of the VHB elastomer. For a model generator operating in a Carnot-like cycle, we show that the performance parameters are strongly dependent on operating frequencies and strains. The generator is most efficient in fast cycles with relatively small operating strains. For long cycle durations, the generator may operate at negative efficiency and waste energy due to substantial leakage losses. Viscous losses also increase the mechanical input work, which results in a lower efficiency for the generator. We also find that the generator may achieve high specific energy density and specific power by operating in fast cycles under large strains. However for slower cycles, the performance of the generator diminishes under larger operating strains due to significant current leakage losses. Our method may be adapted to analyze more sophisticated generator designs and material models, with different cycles of operation and operating conditions. This method may be used to evaluate, design, and optimize dielectric elastomer generators.

ACKNOWLEDGMENTS

The work at Harvard is supported by ARO (W911NF-09-1-0476) and MRSEC. CC Foo acknowledges A*STAR, Singapore for sponsoring his visit to Harvard University. S. J. A. Koh acknowledges the start-up funding from Ministry of Education (Singapore), administered through the National University of Singapore. S.B. gratefully acknowledges financial support from the Austrian Science Funds and from the European Research Council.

- ¹R. Pelrine, R. Kornbluh, Q. Pei, and J. Joseph, *Science* **287**, 836–839 (2000).
- ²F. Carpi, S. Bauer, and D. De Rossi, *Science* **330**, 1759–1761 (2010).
- ³R. Pelrine, R. D. Kornbluh, J. Eckerle, P. Jeuck, S. Oh, Q. Pei, and S. Stanford, *Proc. SPIE* **4329**, 148 (2001).
- ⁴S. J. A. Koh, C. Keplinger, T. Li, S. Bauer, and Z. Suo, *IEEE/ASME Trans. Mechatron.* **16**, 33–41 (2011).
- ⁵R. D. Kornbluh, R. Pelrine, H. Prahla, A. Wong-Foy, B. McCoy, S. Kim, J. Eckerle, and T. Low, *Proc. SPIE* **7976**, 797605 (2011).
- ⁶J. A. Paradiso and T. Starner, *IEEE Pervasive Comput.* **4**, 18–27 (2005).
- ⁷S. Chiba, M. Waki, R. Kornbluh, and R. Pelrine, *Proc. SPIE* **6927**, 692715 (2008).
- ⁸T. McKay, B. O'Brien, E. Calius, and I. Anderson, *Appl. Phys. Lett.* **97**, 062911 (2010).
- ⁹T. McKay, B. O'Brien, E. Calius, and I. Anderson, *Smart Mater. Struct.* **19**, 055025 (2010).
- ¹⁰T. G. McKay, B. M. O'Brien, E. P. Calius, and I. A. Anderson, *Appl. Phys. Lett.* **98**, 142903 (2011).
- ¹¹C. Jean-Mistral, S. Basrour, and J.-J. Chaillout, *Proc. SPIE* **6927**, 692716 (2008).
- ¹²M. Jean, *Smart Mater. Struct.* **19**, 085012 (2010).
- ¹³J.-S. Plante and S. Dubowsky, *Sens. Actuators, A* **137**, 96–109 (2007).
- ¹⁴C. Graf and J. Maas, *Proc. SPIE* **7642**, 764217 (2010).
- ¹⁵R. Kaltseis, C. Keplinger, R. Baumgartner, M. Kaltenbrunner, T. Li, P. Mächler, R. Schwödiauer, Z. Suo, and S. Bauer, *Appl. Phys. Lett.* **99**, 162904 (2011).
- ¹⁶C. C. Foo, S. Q. Cai, S. J. A. Koh, S. Bauer, and Z. Suo, *J. Appl. Phys.* **111**, 034102 (2012).
- ¹⁷X. Zhao, W. Hong, and Z. Suo, *Phys. Rev. B* **76**, 134113 (2007).
- ¹⁸D. A. Seanor, *Adv. Polym. Sci.* **4**, 317–352 (1965).
- ¹⁹G. G. Raju, in *Dielectrics in Electric Fields* (Marcel Dekker, New York, 2003), pp. 329–382.
- ²⁰L. Di Lillo, A. Schmidt, A. Bergamini, P. Ermanni, and E. Mazza, *Proc. SPIE* **7976**, 79763 (2011).
- ²¹J. Plante and S. Dubowsky, *Int. J. Solids Struct.* **43**, 7727–7751 (2006).
- ²²X. Zhao, S. J. A. Koh, and Z. Suo, *Int. J. Appl. Mech.* **3**, 1–15 (2011).
- ²³W. Hong, *J. Mech. Phys. Solids* **59**, 637–650 (2011).
- ²⁴A. N. Gent, *Rubber Chem. Technol.* **69**, 59–61 (1996).
- ²⁵S. Michel, X. Q. Zhang, M. Wissler, C. Löwe, and G. Kovacs, *Polym. Int.* **59**, 391–399 (2009).
- ²⁶M. Wissler and E. Mazza, *Sens. Actuators, A* **134**, 494–504 (2007).
- ²⁷S. J. A. Koh, X. Zhao, and Z. Suo, *Appl. Phys. Lett.* **94**, 262902 (2009).
- ²⁸H. U. Fuchs, *Am. J. Phys.* **54**, 907 (1986).
- ²⁹F. L. Curzon and B. Ahlborn, *Am. J. Phys.* **43**, 22 (1975).
- ³⁰G. Kofod, P. Sommer-Larsen, R. Kornbluh, and R. Pelrine, *J. Intell. Mater. Syst. Struct.* **14**, 787 (2003).
- ³¹T. A. Gisby, S. Q. Xie, E. P. Calius, and I. A. Anderson, *Proc. SPIE* **7642**, 764213 (2010).
- ³²R. Pelrine and H. Prahla, in *Dielectric Elastomers as Electrochemical Transducers* (Elsevier, Amsterdam, 2008), pp. 146–155.